AERODYNAMIC LOADS ON DEVICES FOR SIMULATING INLET/ENGINE FLOW CONDITIONS AND EFFECTS OF TEST INSTALLATION ON TUNNEL OPERATION

PROPULSION WIND TUNNEL FACILITY
ARNOLD ENGINEERING DEVELOPMENT CENTER
AIR FORCE SYSTEMS COMMAND
ARNOLD AIR FORCE STATION, TENNESSEE 37389

July 1975

Final Report for Period July 1974 – February 1975

Prepared for

DIRECTORATE OF CIVIL ENGINEERING
ARNOLD ENGINEERING DEVELOPMENT CENTER
ARNOLD AIR FORCE STATION, TENNESSEE 37389

NOTICES

When U. S. Government drawings specifications, or other data are used for any purpose other than a definitely related Government procurement operation, the Government thereby incurs no responsibility nor any obligation whatsoever, and the fact that the Government may have formulated, furnished, or in any way supplied the said drawings, specifications, or other data, is not to be regarded by implication or otherwise, or in any manner licensing the holder or any other person or corporation, or conveying any rights or permission to manufacture, use, or sell any patented invention that may in any way be related thereto.

Qualified users may obtain copies of this report from the Defense Documentation Center.

References to named commercial products in this report are not to be considered in any sense as an endorsement of the product by the United States Air Force or the Government.

This report has been reviewed by the Information Office (OI) and is releasable to the National Technical Information Service (NTIS). At NTIS, it will be available to the general public, including foreign nations.

APPROVAL STATEMENT

This technical report has been reviewed and is approved for publication.

FOR THE COMMANDER

CHARLES V. BENNETT
Facility Development Division
Directorate of Civil Engineering

ROLAND R. GARREN
Colonel, USAF
Director of Civil Engineering

REPORT DOCUMENTATION PAGE		READ INSTRUCTIONS BEFORE COMPLETING FORM
1 REPORT NUMBER AEDC-TR-75-74	2. GOVT ACCESSION NO.	3. RECIPIENT'S CATALOG NUMBER
4. TITLE (and Subtitle) AERODYNAMIC LOADS ON DEVICES FOR SIMULATING INLET/ENGINE FLOW CONDITIONS AND EFFECTS OF TEST INSTALLATION ON TUNNEL OPERATION		5. TYPE OF REPORT & PERIOD COVERED Final Report - July 1974 February 1975 6. PERFORMING ORG. REPORT NUMBER
7. AUTHOR(s) R. L. Palko - ARO, Inc.		8. CONTRACT OR GRANT NUMBER(s)
9. PERFORMING ORGANIZATION NAME AND ADDRESS Arnold Engineering Development Center (XO) Arnold Air Force Station (DE) Tennessee 37389		10. PROGRAM ELEMENT, PROJECT, TASK AREA & WORK UNIT NUMBERS Program Element 65802F
11. CONTROLLING OFFICE NAME AND ADDRESS Arnold Engineering Development Center (DYFS), Arnold Air Force Station, Tennessee 37389		12. REPORT DATE July 1975 13. NUMBER OF PAGES 32
14. MONITORING AGENCY NAME & ADDRESS (if different from Controlling Office)		15. SECURITY CLASS. (of this report) UNCLASSIFIED 15a. DECLASSIFICATION/DOWNGRADING SCHEDULE N/A

16. DISTRIBUTION STATEMENT (of this Report)

Approved for public release; distribution unlimited.

17. DISTRIBUTION STATEMENT (of the abstract entered in Block 20, if different from Report)

18. SUPPLEMENTARY NOTES

Available in DDC.

19. KEY WORDS (Continue on reverse side if necessary and identify by block number)

transonic wind tunnels
test facilities
inlet/engine systems
angle of attack
transonic flow
flow-shaping devices
aerodynamic loading

20. ABSTRACT (Continue on reverse side if necessary and identify by block number)

Aerodynamic loads were experimentally determined using 1/16-scale models of the flow-shaping device configurations to be used with the newly developed flow-shaping technique for testing full-scale inlet/engine systems in the AEDC 16-ft Propulsion Wind Tunnel (Transonic) at high angles of attack and at combinations of angle of attack and angle of yaw. The wind tunnel operating characteristics and performance limitations with the inlet/engine

DD FORM 1 JAN 73 1473 EDITION OF 1 NOV 65 IS OBSOLETE

20. ABSTRACT (Continued)

and the flow-shaping devices installed were also determined. All data are now available to design the support equipment for a workable system capable of providing simulation of flight attitudes from 0- to 20-deg angle of attack with 0-deg yaw angle, and from 0- to 8-deg angle of attack at yaw angles from -6 to 6 deg over the Mach number range from 0.6 to 0.9.

AFSC
Arnold AFS Tenn

PREFACE

The work reported herein was conducted by the Arnold Engineering Development Center (AEDC), Air Force Systems Command (AFSC), under Program Element 65802F. Technical monitoring of the effort was performed by Mr. W. R. Bates, Facility Development Division, Directorate of Civil Engineering. The results presented were obtained by ARO, Inc. (a subsidiary of Sverdrup & Parcel and Associates, Inc.), contract operator of AEDC, AFSC, Arnold Air Force Station, Tennessee. The investigation was conducted under ARO Project Nos. P37A-45A and P41A-01A. The author of this report was R. L. Palko, ARO, Inc. The manuscript (ARO Control No. ARO-PWT-TR-75-38) was submitted for publication on April 4, 1975.

Acknowledgment is made of the contributions of Mr. W. P. Harmon of the Propulsion Wind Tunnel Facility, Test Operations Branch, who designed the balance and test equipment, and Mr. J. A. Reed of the Propulsion Wind Tunnel Facility, 16T/S Projects Branch, who assisted during the wind tunnel entry.

CONTENTS

ILLUSTRATIONS

Figure Page

TABLES

APPENDIX

1.0 INTRODUCTION

A new testing technique has been under development in the 1-ft Aerodynamic Wind Tunnel (transonic) (PWT-1T) at AEDC that will allow testing of full-scale inlet/engine systems in the 16-ft Propulsion Wind Tunnel (transonic) (PWT-16T) at angles of attack up to 20 deg and angles of yaw up to ±6 deg. This development effort has resulted in a feasible technique which utilizes two flow-shaping configurations, one on each side of the inlet, to change the local flow direction and Mach number to match the flow direction and Mach number for conditions at higher angle of attack or yaw. The results of this development effort are reported in Refs. 1 through 6.

To operate these devices efficiently during an inlet/engine test will require that they be remotely variable in rotational angle, in lateral and vertical translation, and in yaw angle. To size the support system and design a mechanism to provide remote control requires an accurate knowledge of the aerodynamic loads and moments on the shaping devices during tunnel operation. Preliminary calculations showed these loads and moments to be very high. These estimated loads were questionable since it was impossible to allow for the interaction between the flow-shaping devices themselves and between the shaping devices and the inlet. Therefore, a wind tunnel test was conducted with scale models of the devices and inlet in the PWT-1T to experimentally determine the aerodynamic loads. Loads and moments were measured on one of the flow-shaping devices using a 5-component sidewall balance. Three shapes were tested on the balance at two yaw angles and at rotational angles over the range from 0 to 30 deg. Mach number was varied from 0.6 to 0.9 at these angles to match the conditions required to simulate the test conditions given in Refs. 4 and 6.

Reference 3 recommended the addition of tunnel plenum pumping capacity for PWT-16T if the technique was to be used. However, this reference indicated that limited performance could be obtained with the present Plenum Evacuation System (PES). During the present test effort, measurements were made to determine the wind tunnel operating characteristics and performance capability, based on the conditions required for the simulations reported in Refs. 4 and 6.

Results of the aerodynamic loads study and the wind tunnel operating characteristics are reported herein.

2.0 APPARATUS

2.1 WIND TUNNEL (AEDC PWT-1T)

Tunnel 1T is a continuous-flow, nonreturn, transonic wind tunnel equipped with a two-dimensional, flexible nozzle and a plenum evacuation system. The test section Mach number range can normally be varied from 0.2 to 1.50. Total pressure control is not available, and the tunnel is operated at a stilling chamber total pressure of about 2850 psfa with a ±5-percent variation depending on tunnel resistance and ambient conditions. Stagnation temperature can be varied from 80 to 120°F above ambient temperature when necessary to prevent moisture condensation in the test region.

The PWT-1T represents a one-sixteenth scale model of the critical aerodynamic sections of the PWT-16T with the test section rotated 90 deg. The general arrangement of the tunnel and its associated equipment is shown in Fig. 1, and a schematic of the nozzle, test section, and wall geometry is shown in Fig. 2.

The plenum suction line has a flow-metering orifice for measuring the plenum suction requirements during tunnel blockage studies. This orifice is located in the line as shown in Fig. 1.

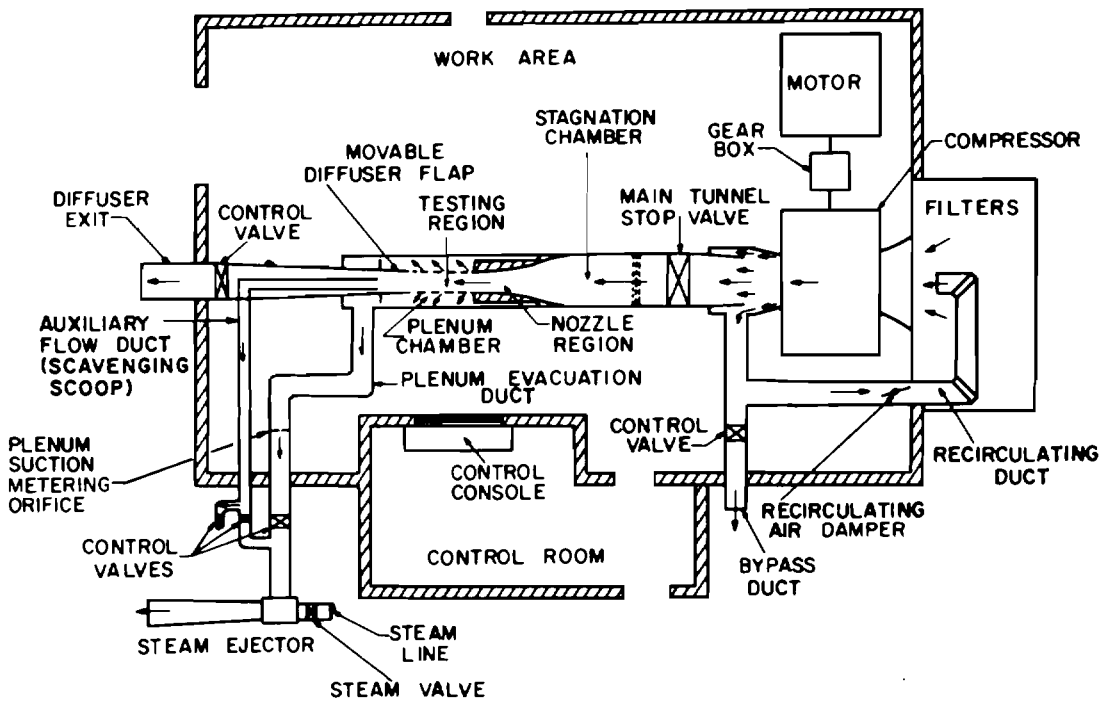

Figure 1. General arrangement of the AEDC PWT-1T and supporting equipment.

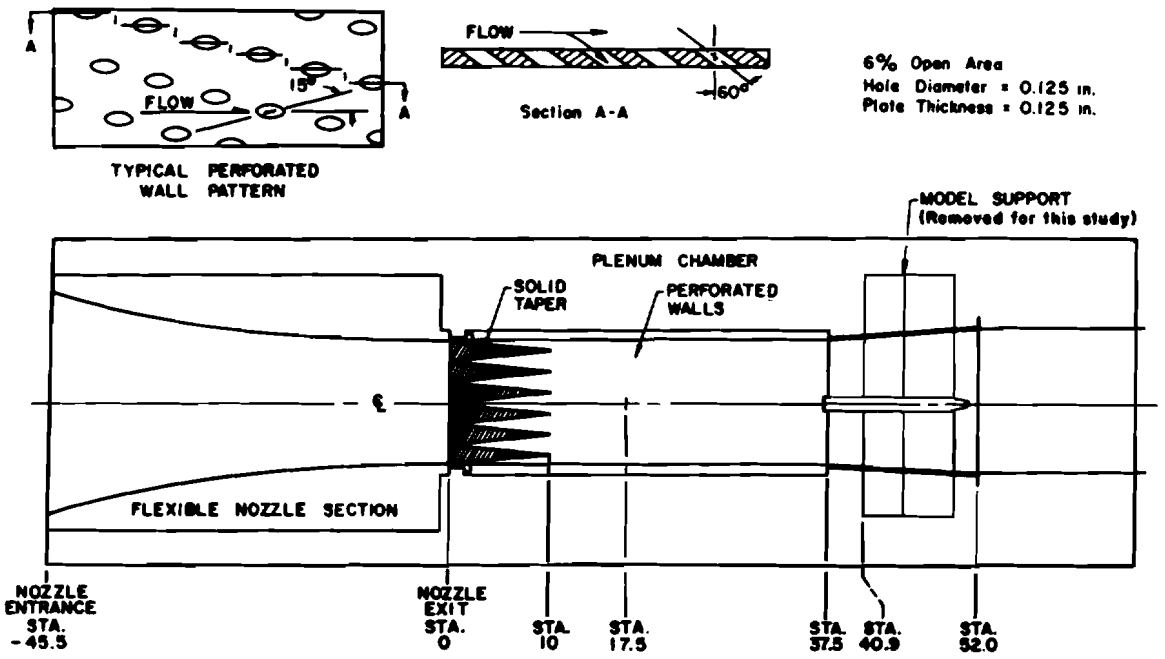

Figure 2. Schematic of the AEDC PWT-1T test leg.

2.2 FLOW-SHAPING DEVICES

The basic flow-shaping device consisted of two hollow, half-circular cylinders which were split and widened in the middle by the width of one radius. Two variations to this configuration were also used, one with a built-in 5-deg positive yaw and one with a built-in 5-deg negative yaw. The shape and reference dimensions of these flow-shaping devices are shown in Fig. 3.

One cylinder (Cylinder No. 1) was attached to a 5-component, sidewall, moment-type balance that was designed and fabricated specifically for this study. Force and moment data could be obtained only from this position. Therefore, each skin was run on this base to obtain the data. (This cylinder corresponds to the left side device when looking downstream in PWT-16T.) A sketch of the balance and cylinder attachment is shown in Fig. 4. The balance support could be yawed to a positive 10 deg which yawed the cylinder in the wind tunnel by the same amount. Rotation angle was set utilizing a serrated face attachment between the cylinder and balance strut which allowed angles from 0 to 30 deg to be set in 5-deg increments.

The bottom wall-mounted device (Cylinder No. 2), which corresponds to the right side device when looking downstream in PWT-16T, could be remotely rotated through a continuous angle range from 0 to 35 deg. Lateral position of this cylinder, from the tunnel wall, could also be remotely controlled, although for this study the position was held constant.

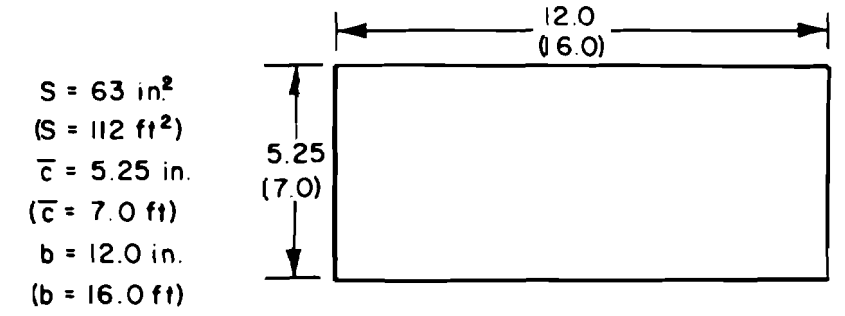

a. Base view and reference dimensions

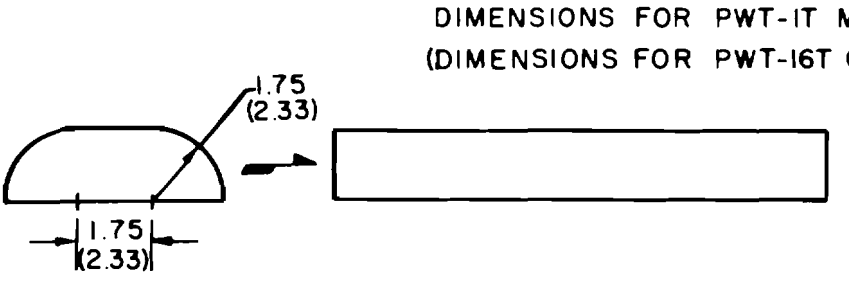

b. Front and side views of base configuration (MC)

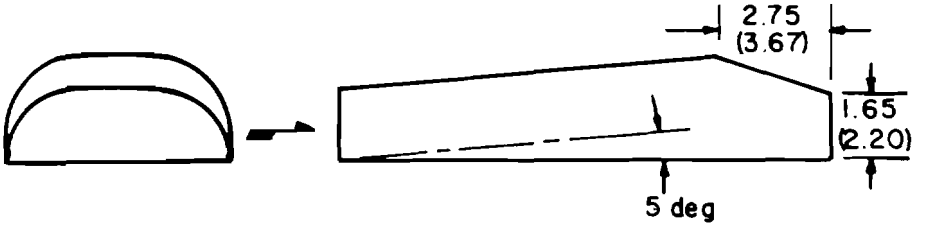

c. Front and side views of 5-deg positive yaw configuration (1MMC2)

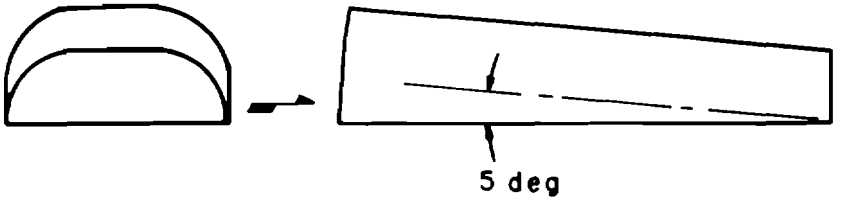

d. Front and side views of 5-deg negative yaw configuration (2MMC)

Figure 3. Schematic of flow-shaping devices.

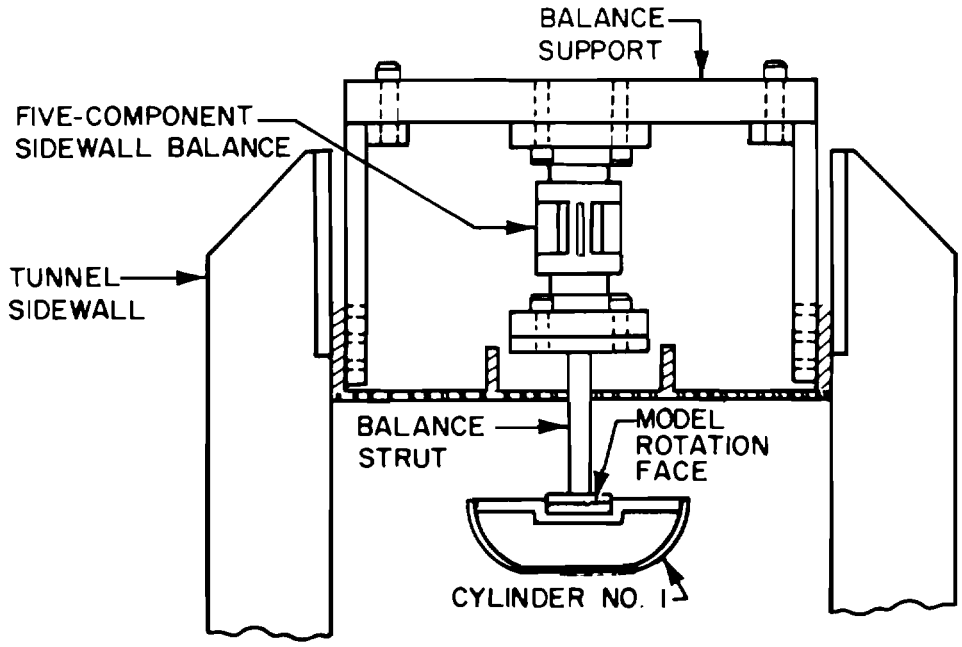

a. Front view

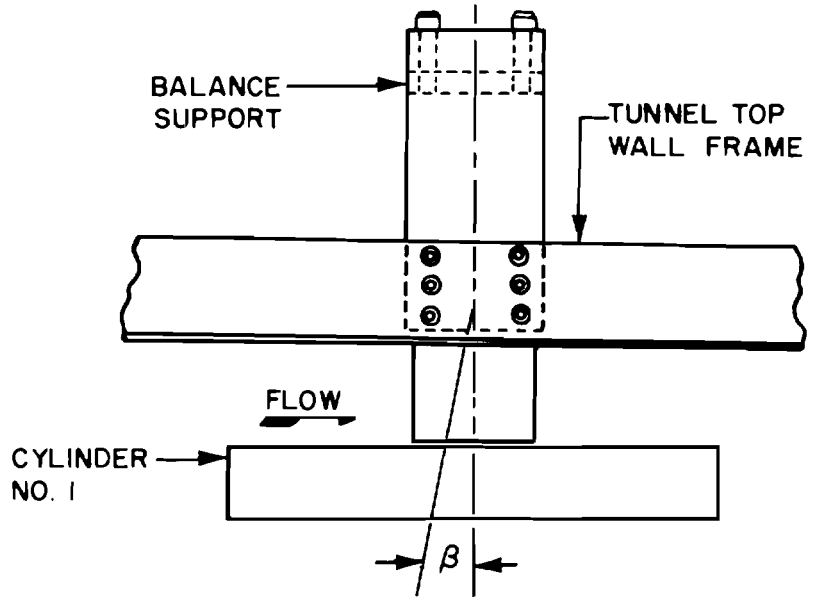

b. Side view

Figure 4. Schematic of balance installation.

2.3 INLET MODEL

The inlet model used was a 1/16-scale, two-dimensional, supersonic inlet available from a previous wind tunnel blockage study. This was the same model used during the development of the test technique as reported in Refs. 1 through 6. The inlet angle of attack could be manually set from 0 to 12 deg in 2-deg increments. Relative position of the inlet and flow-shaping devices is shown schematically in Fig. 5. Photographs of the tunnel installation are shown in Figs. 6 and 7.

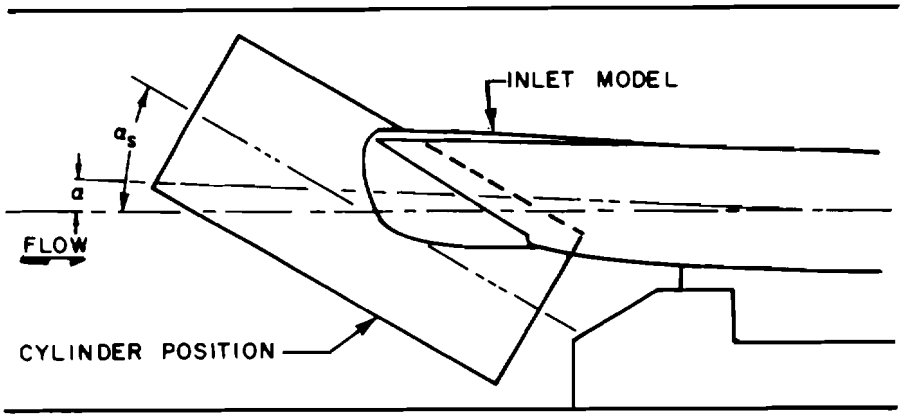

a. Bottom view (viewed as the installation would appear from the side in the PWT-16T)

DIMENSIONS FOR PWT-1T IN INCHES
(DIMENSIONS FOR PWT-16T IN FEET)

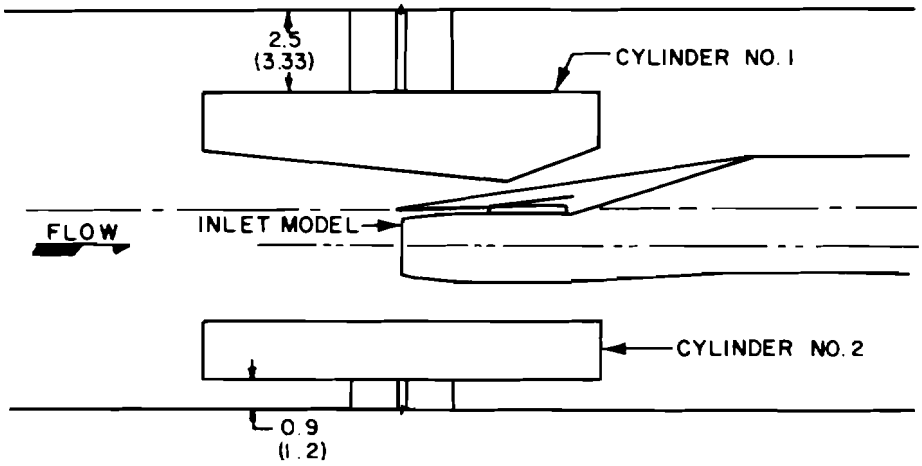

b. Side view (viewed as the installation would appear from the top in the PWT-16T)

Figure 5. Schematic of the model installation in the PWT-1T.

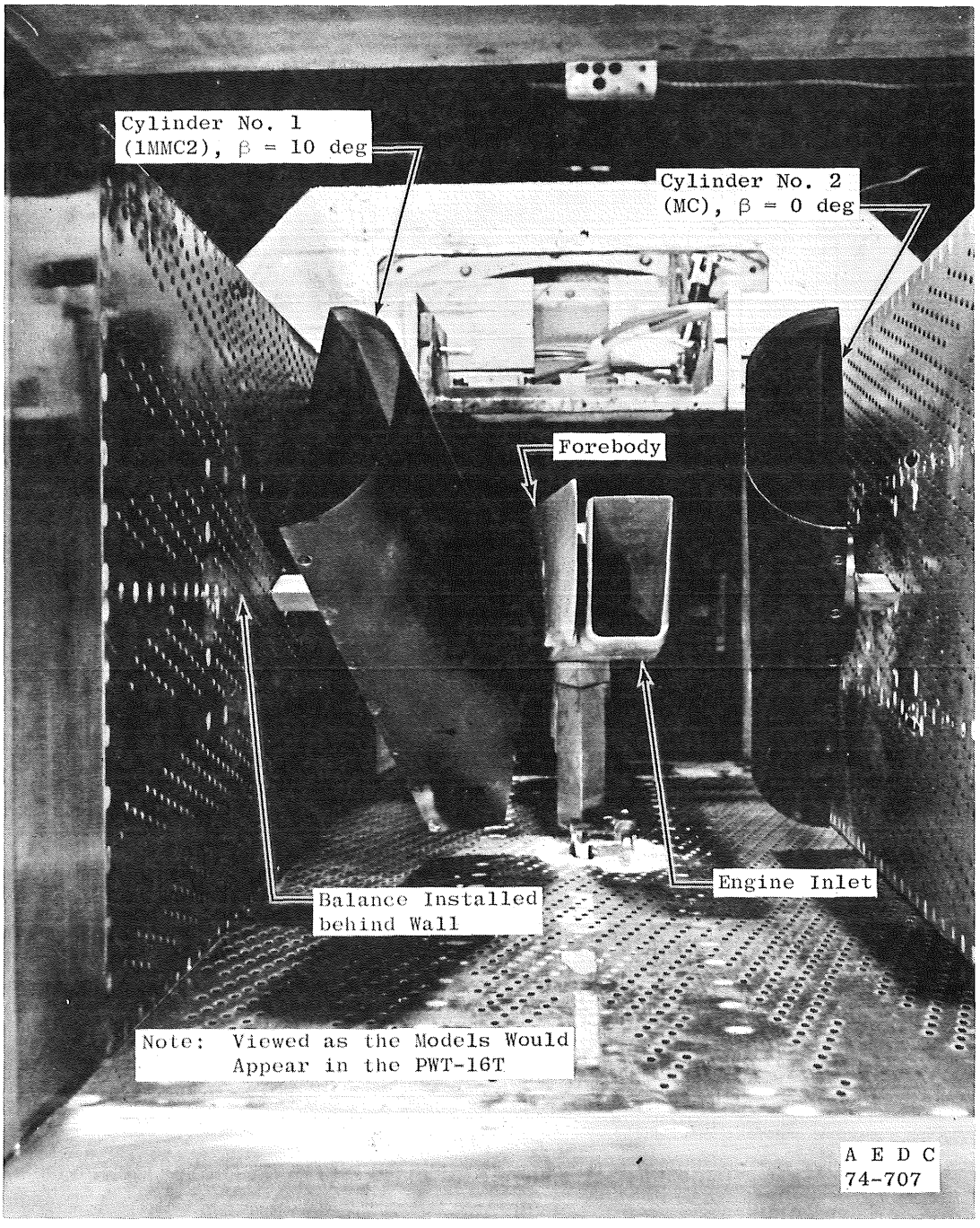

Figure 6. Front view of flow-shaping devices and inlet model installed in PWT-1T.

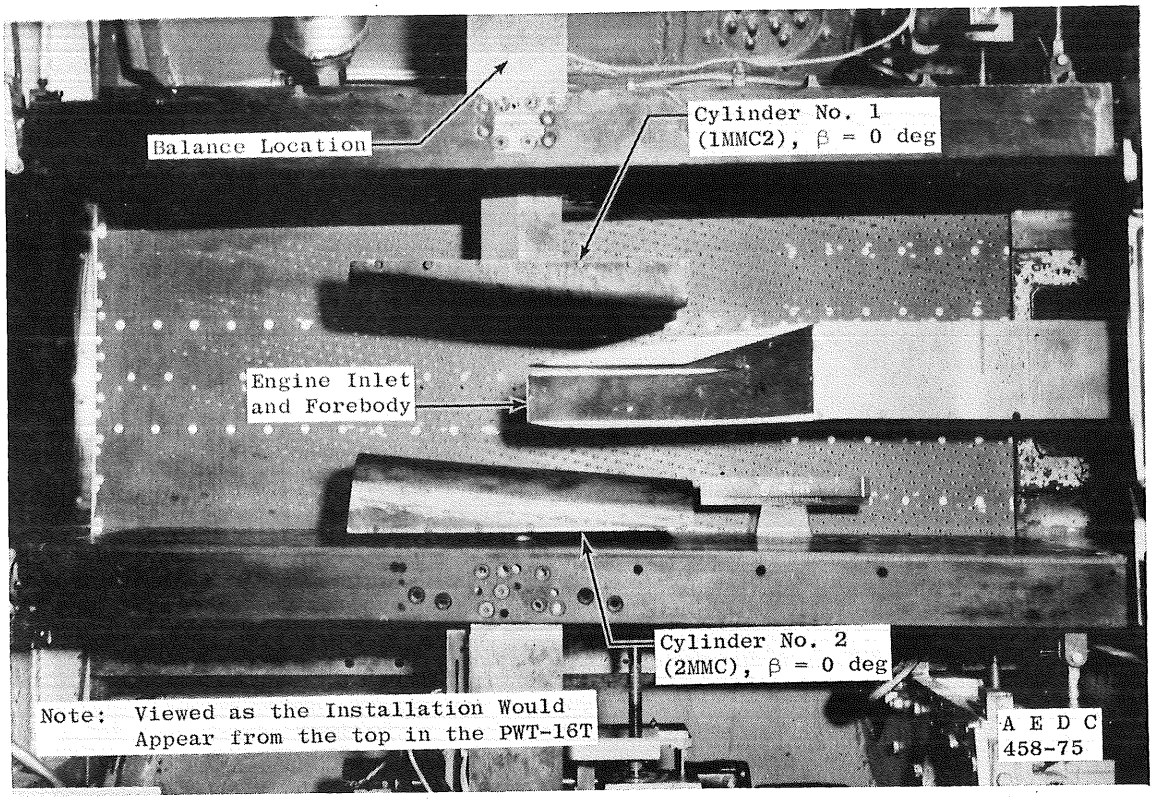

Figure 7. Side view of flow-shaping devices and inlet model installed in PWT-1T.

2.4 INSTRUMENTATION AND DATA ACQUISITION SYSTEMS

Tunnel 1T is equipped with a permanently installed, automatic data recording system. A PDP 11-20 computer provides on-line data reduction. Reduced data are displayed on a line printer, and a high-speed paper tape punch records and stores the raw data for the purpose of later off-line analysis. Pressure data are measured with differential pressure transducers referenced to the tunnel plenum pressure. Analog signals from the pressure transducers and from the balance strain gages are fed through a switch gain amplifier and then through an analog-to-digital (A-D) converter to be digitized. The A-D converter used 12 bits plus sign, or 4096 counts full scale, and the digital signals from the converter are processed by the PDP 11-20 computer.

Maximum uncertainties in the data, taking into account the inaccuracies in the balance and pressure measurements, were calculated to be as follows:

M_∞	Q	P_t	C_N	C_A	C_m	C_n	C_ℓ
±0.005	±5.4 psf	±1.3 psf	±0.005	±0.004	±0.002	±0.002	±0.002

3.0 RESULTS AND DISCUSSION

3.1 AERODYNAMIC FORCES

Aerodynamic forces and moments were measured on the top wall-mounted flow-shaping device (Cylinder No. 1) while in the proximity of the inlet/engine and the bottom wall-mounted flow-shaping device (Cylinder No. 2) while installed in the PWT-1T. The purpose of the test was to obtain the necessary loads for design of a flow-shaping system for use in PWT-16T during full-scale inlet/engine testing. One-sixteenth scale models were used for the test, with two components of force (normal and axial) and three moments (pitching, yawing, and rolling) measured as shown in Fig. 8. Side force was not measured; however, the side force acts as a compression load on the support strut and, therefore, was not considered to be a problem.

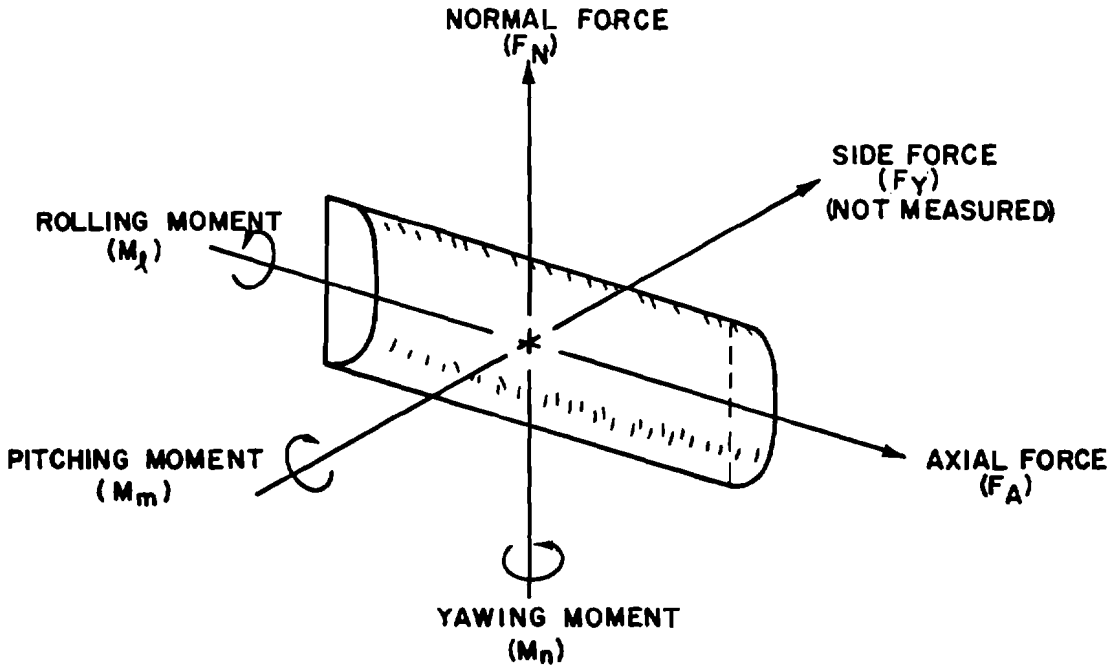

Figure 8. Schematic of axis system for forces and moments on the flow-shaping device (Cylinder No. 1).

Loads on three different flow-shaping device configurations (see Fig. 3) were measured over the Mach number range from 0.6 to 0.9. A comparison of the force and moment coefficients for the three configurations at a Mach number of 0.9 (Data from which critical loads where determined, see Table 1 for reference figure, show Mach 0.9 gave the highest loads for all components) is shown in Fig. 9. The coefficients are plotted as a function of cylinder rotation angle, while the inlet/engine model angle of attack was 2 deg and the inlet mass flow

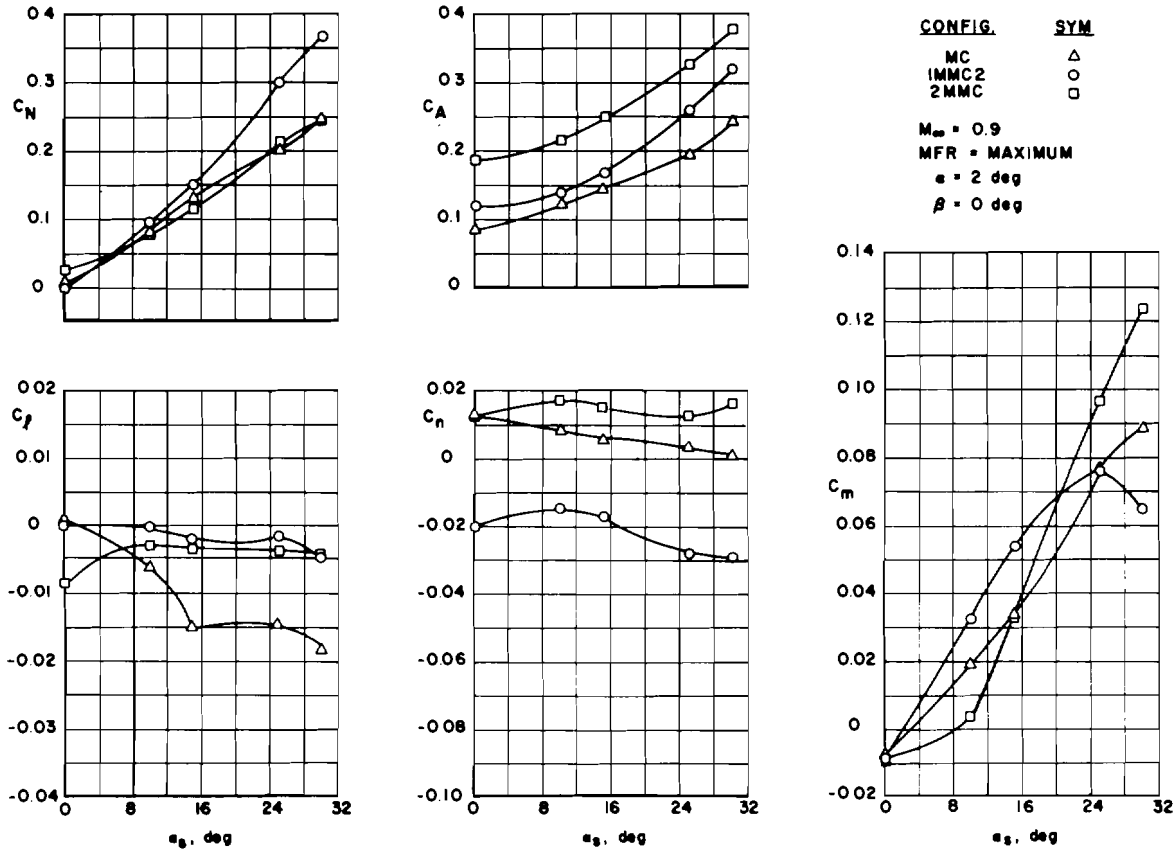

Figure 9. Comparison of force and moment coefficients for three skin shape configurations.

ratio (MFR) was set for maximum flow. Normal force and axial force exhibited smooth increases with increasing rotational angle. The 5-deg positive yaw configuration (1MMC2) had a higher normal-force coefficient (C_N) by a ΔC_N = 0.120, while the other two configurations exhibited approximately the same C_N. Variation in axial-force coefficient (C_A) among the three configurations was more consistent. The 5-deg negative yaw configuration (2MMC) had a consistently higher value than the other two configurations, with a ΔC_A = 0.055 from the 1MMC2 configuration, and a ΔC_A = 0.130 from the base configuration (MC). Moment coefficients had less uniform trends due to the shifting of the center-of-pressure (CP) on the cylinder as a result of the flow interaction between the shaping devices and inlet/engine model. The MC configuration had the highest rolling-moment coefficient (C_ℓ) by a ΔC_ℓ = 0.135 at α_s = 30 deg. The 1MMC2 configuration had the highest yawing-moment coefficient (C_n) with a value of -0.029 at α_s = 30 deg; however, the 2MMC configuration had a C_n = +0.017 at α_s = 10 deg. The 2MMC configuration had the highest pitching-moment coefficient (C_m) by a ΔC_m = 0.035 over the MC configuration and a ΔC_m = 0.059 over the 1MMC2 configuration.

Effect of Mach number on the forces and moments is shown in Fig. 10 for the 1MMC2 configuration. (Corresponding data for the other two configurations, plus the 1MMC2 and MC configurations at β = 10 deg, are included in Appendix A.) Normal force and axial force both show a general increase with Mach number which is representative of data for all configurations tested. However, here again the moment data are not as uniform. For this particular configuration, the Mach 0.6 data show the highest moment coefficients which is the basic trend (with few exceptions) for all configurations.

Effects of the inlet mass flow ratio (MFR) on the force and moment coefficients, for the 1MMC2 configuration, are shown in Fig. 11. Varying MFR had little or no effect on the forces and moments with the exception of the pitching moment which shows some effect. The MFR $\approx$ 0.7 condition had a ΔC_m = 0.011 increase at α_s = 25 deg over the MFR $\approx$ 0.3 condition.

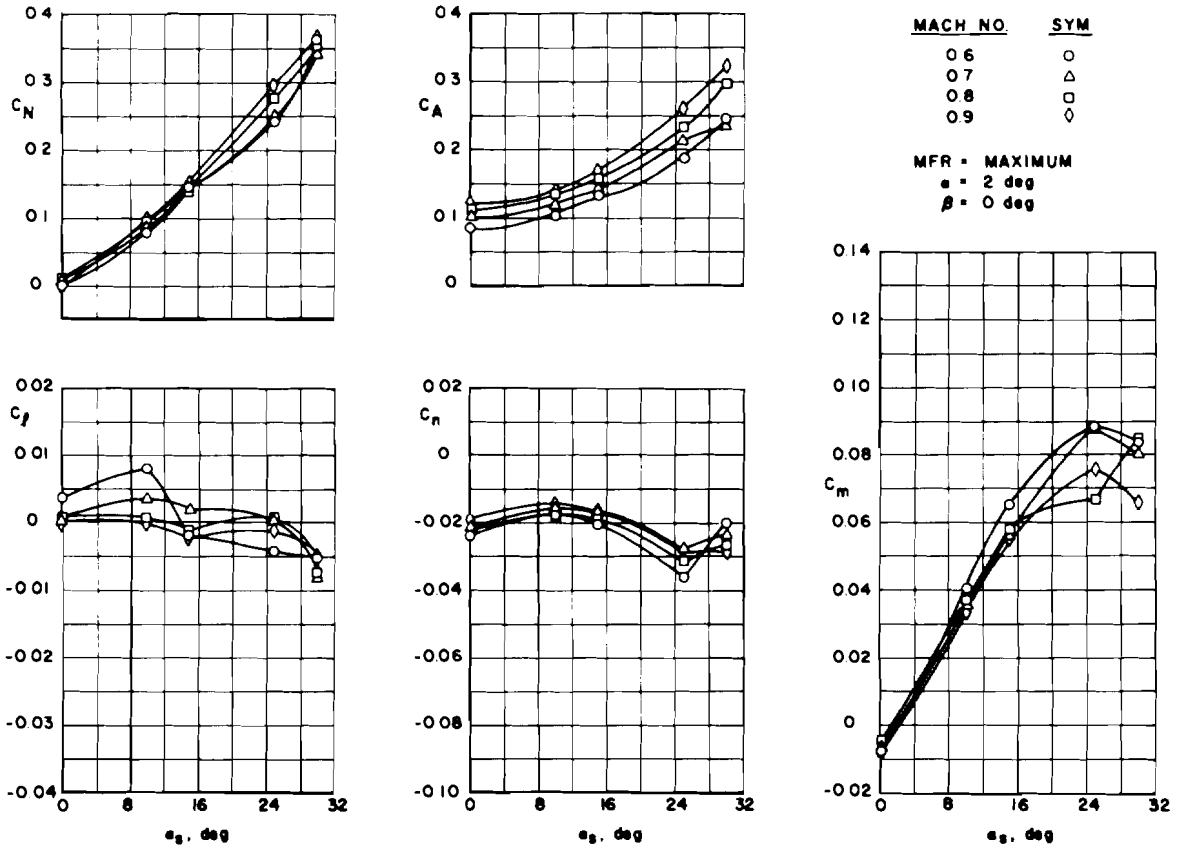

Figure 10. Effect of Mach number on the force and moment coefficients with the 1MMC2 configuration.

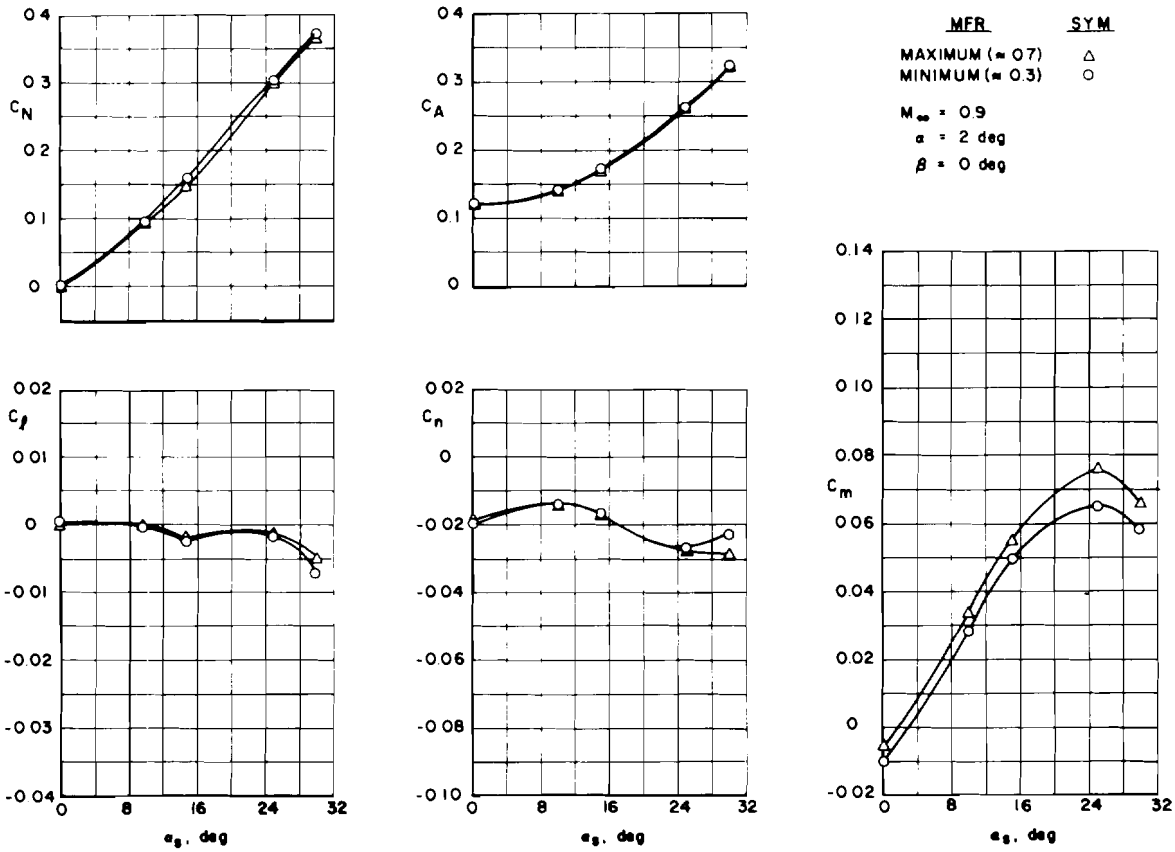

Figure 11. Effect of the inlet mass flow ratio on the force and moment coefficients with the 1MMC2 configuration.

Effects of the inlet/engine pitch angle on the force and moment coefficients for the 1MMC2 configuration are shown in Fig. 12. The loads measured with the inlet/engine set at 2-deg angle of attack were generally higher for all components except pitching moment which was higher with the inlet/engine set at 10 deg.

Effects of cylinder yaw angle on the force and moment coefficients, for the 1MMC2 configuration, are shown in Fig. 13. Yawing the cylinder to +10 deg had a significant effect on the C_N, C_n, and C_m. The C_N was increased by approximately 0.07 over the cylinder rotation range from 10 to 25 deg, while C_n was increased by a factor of 4 at α_s = 0 deg, and more than doubled at α_s = 30 deg. The C_m was a negative 0.02 at α_s = 0 deg with β = 10 deg, whereas C_m was approximately zero at α_s = 0 deg with β = 0 deg. The C_m curves slope toward each other and intersect at approximately α_s = 25 deg, where the C_n for β = 0 deg starts to decrease and the C_m for β = 10 deg continues to increase in a uniform manner up to C_m = 0.095.

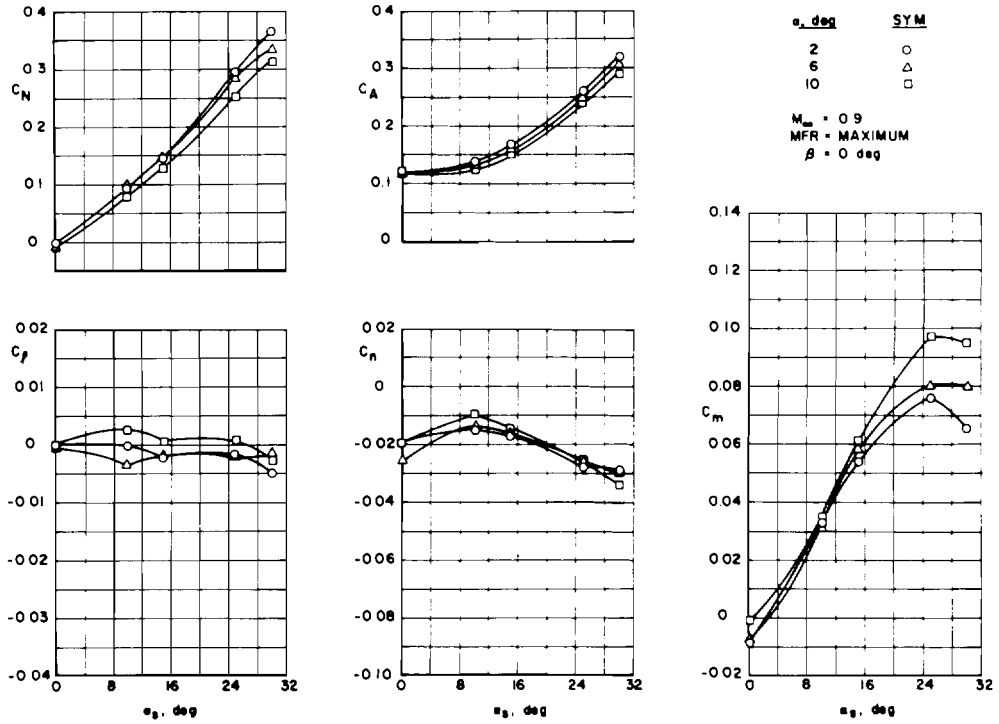

Figure 12. Effect of inlet pitch angle on the force and moment coefficients with the 1MMC2 configuration.

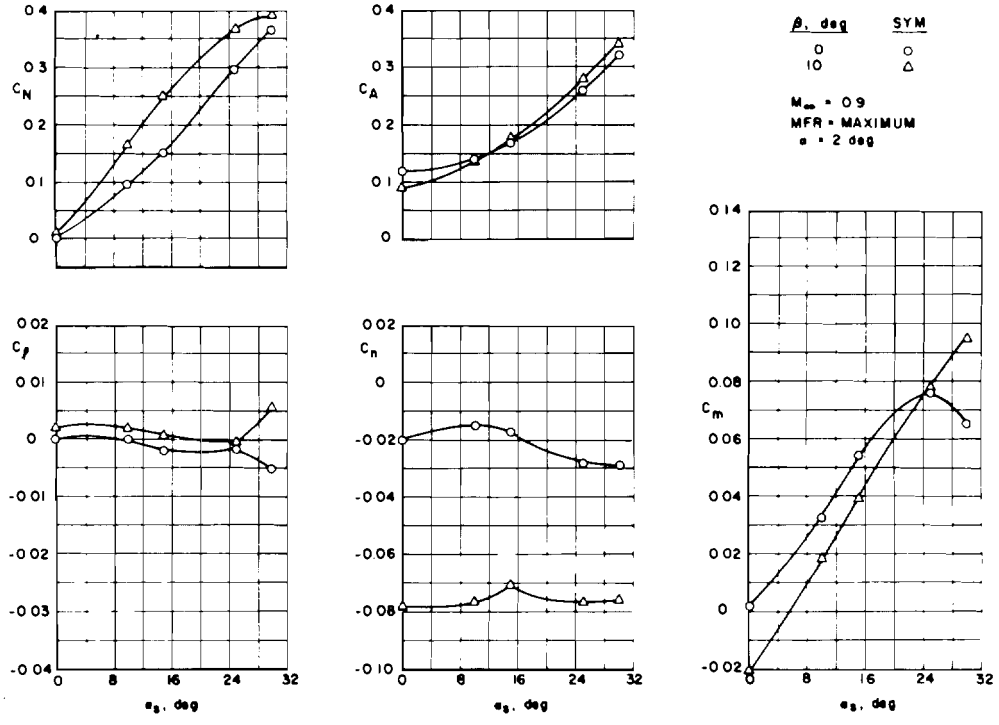

Figure 13. Effect of cylinder yaw angle on the force and moment coefficients with the 1MMC2 configuration.

Effects of cylinder yaw angle on the force and moment coefficients for the MC configuration are shown in Fig. 14. Significant effects are present on all components with this configuration. However, the most significant effect is still the effect on C_n where the ΔC_n between the β = 0 deg and β = 10 deg yaw positions was as high as 0.055. A crossover of the data is shown for both C_A and C_m at α_s = 14 deg.

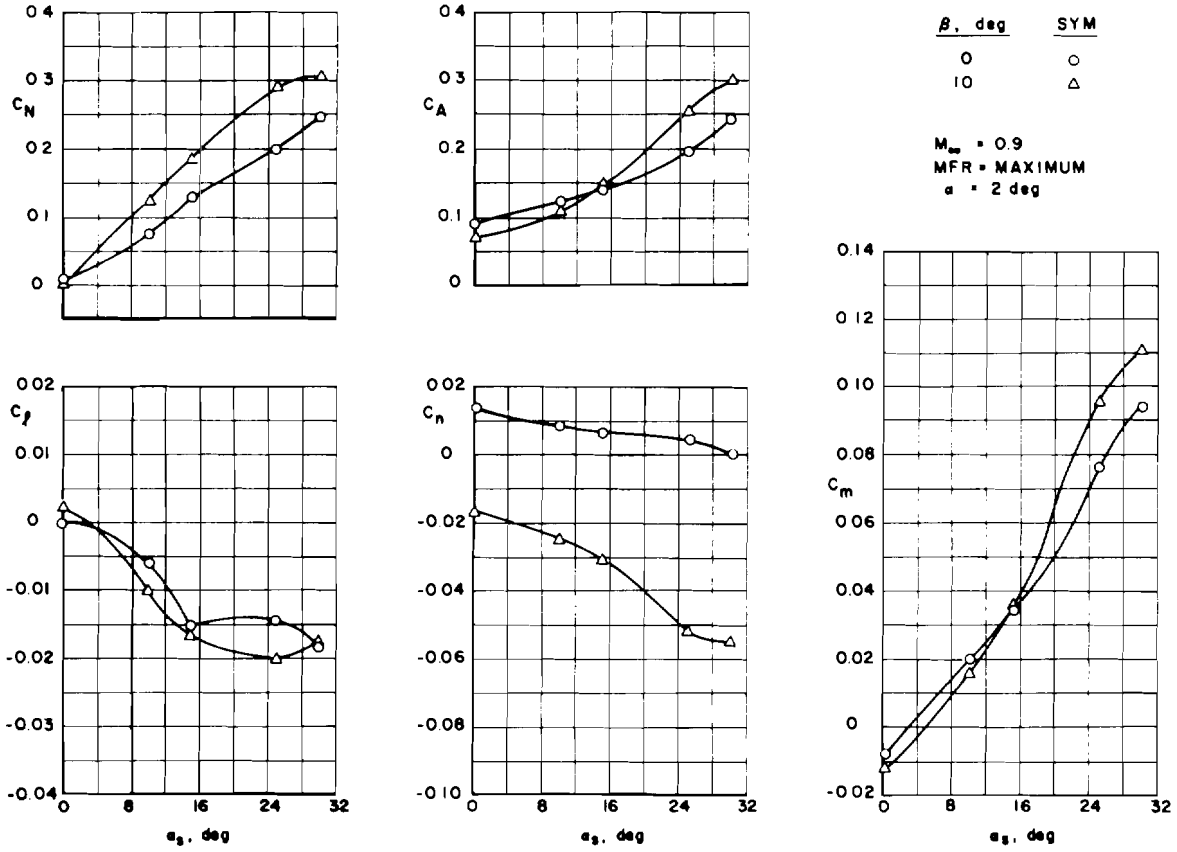

Figure 14. Effect of cylinder yaw angle on the force and moment coefficients with the MC configuration.

A check of the data repeatability is shown in Fig. 15. These data are for the MC configuration with α_s = 15 deg, and the coefficients are shown versus Mach number. The C_n values show the largest difference (ΔC_n = 0.003) which is within the data uncertainty, quoted in Section 2.4, of ±0.002.

A summary of the maximum coefficients measured for each component, as well as the corresponding configuration and test conditions, is given in Table 1. Coefficients for the other components that were measured, along with the maximum value, are also given for the combination loads. Forces and moments that result from these configurations for

both PWT-1T and PWT-16T are given in Table 2. The dynamic pressure used in the calculations for both tunnels was 955 psf, with the reference dimensions and Mach number taken from Fig. 3 and Table 1, respectively.

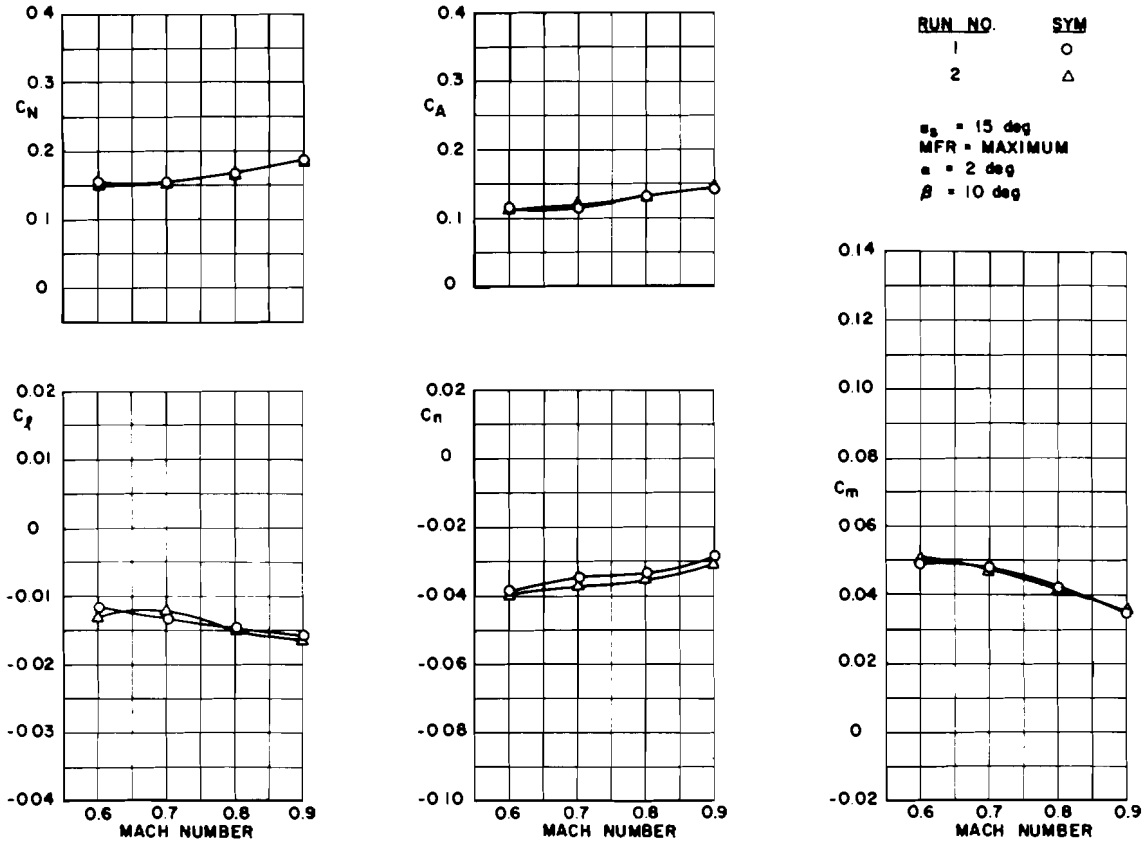

Figure 15. Check of data repeatability with the MC configuration for one rotation angle.

Table 1. Coefficients for Test Conditions that Gave Maximum Measured Coefficient for Each Component in PWT-1T

Maximum Coefficient for ↓	C_N	C_A	C_m	C_n	C_ℓ	Config.	α deg	α_s deg	β deg	M_∞	Ref. Fig.
F_N	0.3900	0.3377	0.0948	-0.0757	0.0056	1MMC2	2	30	10	0.9	A-1
F_A	0.2545	0.3776	0.1238	0.0160	-0.0040	2MMC	2	30	0	0.9	9
M_m	0.2312	0.3667	0.1329	0.0147	-0.0002	2MMC	6	30	0	0.9	A-5
M_n	0.3506	0.2812	0.0835	-0.0910	0.0083	1MMC2	6	25	10	0.9	A-6
M_ℓ	0.2915	0.2561	0.0955	-0.0517	-0.0204	MC	2	25	10	0.9	14 & A-3

Table 2. Load Combinations for Maximum Load on Each Component Based on the Coefficients from Table 1 with a Dynamic Pressure of 955 psf and the Reference Dimensions Given in Figure 3

Maximum for ↓	F_N lb (lb)	F_A lb (lb)	M_m in.-lb (ft-lb)	M_n in.-lb (ft-lb)	M in.-lb (ft-lb)
F_N	165 (41,700)	140 (36,100)	210 (71,000)	-380 (-129,500)	30 (9,600)
F_A	105 (27,200)	160 (40,400)	270 (92,700)	80 (27,400)	-20 (-6,800)
M_m	95 (24,700)	155 (39,200)	290 (99,500)	75 (25,200)	-1 (-300)
M_n	150 (37,500)	120 (30,100)	185 (62,500)	-455 (-155,700)	40 (14,200)
M	120 (31,200)	110 (27,400)	210 (71,500)	-260 (-88,500)	-105 (-35,000)

Measured values from PWT-1T 1/16-scale model test
(Estimated values for PWT-16T full-scale tests)

3.2 WIND TUNNEL OPERATING CHARACTERISTICS AND PERFORMANCE CAPABILITY

Reference 3 showed that additional plenum suction was needed in PWT-16T to use the flow-shaping technique at all desired conditions. To determine the general operating characteristics and limits of the wind tunnel with the flow-shaping equipment and inlet/engine model installed, the plenum suction flow and the wind tunnel pressure ratio were measured during the aerodynamic loads testing. Data were obtained with the flow-shaping devices and the inlet/engine installed with the various configurations and positions corresponding to the flight simulations reported in Refs. 4 and 6. The range of plenum suction weight flow to theoretical tunnel weight flow required for simulation of all the conditions demonstrated in Refs. 4 and 6 is shown in Fig. 16. The figure also shows the performance of the present PWT-PES and the performance gained by additions to the present system. This figure shows that a significant part of the range required to obtain all of the performance at Mach numbers of 0.7, 0.8, and 0.9 is above the present PWT-PES capability. The performance envelope for the test inlet/engine with the present PWT-16T/PES capability is shown in Fig. 17. This figure gives a clearer picture of the limits at each Mach number. The figure shows that the attainable performance envelope for a Mach number of 0.7 is considerably less than for a Mach number of 0.8. This is true for the conditions used in the experimental verification in Ref. 6. It should be noted,

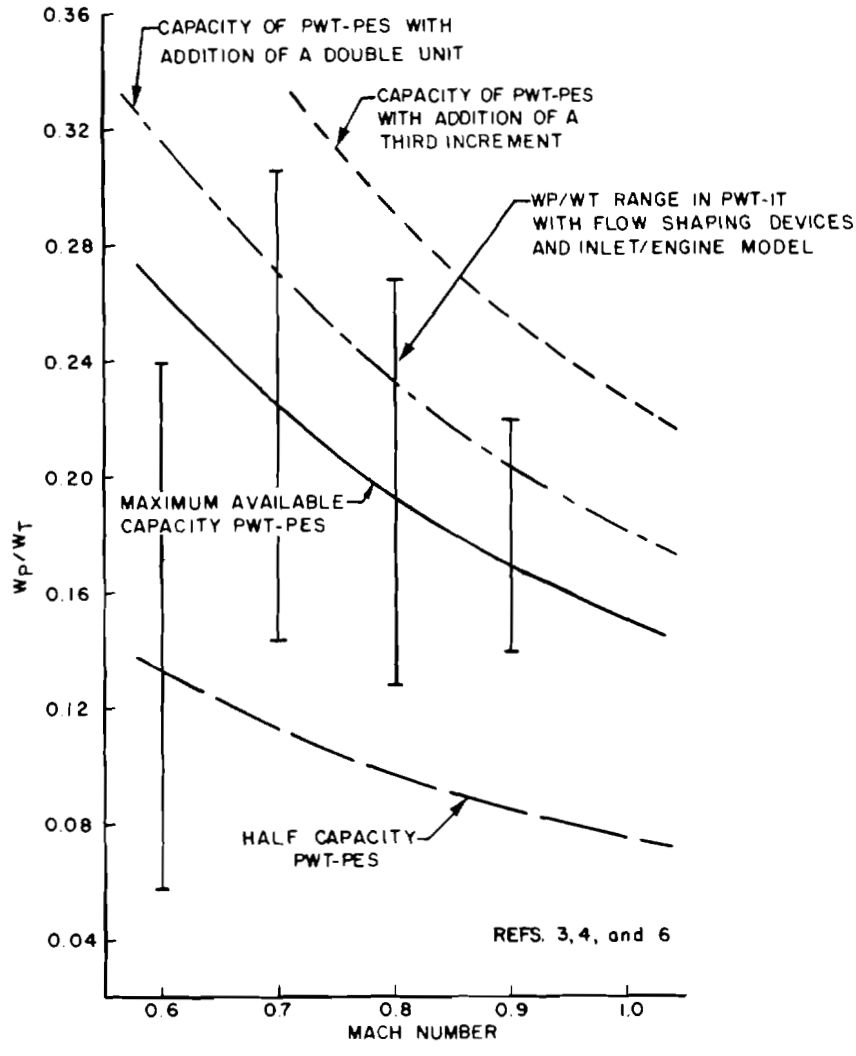

Figure 16. Plenum suction weight flow required to operate the PWT-16T with flow shaping devices and inlet/engine installation.

however, that some of the configurations and positions required for certain simulations were of higher blockage than necessary because of the positioning limits (two-degrees-of-freedom) of the subscale systems. The proposed full-scale system would have four-degrees-of-freedom which will allow better positioning. Better positioning decreases the blockage and should shift the plenum suction requirements down for some conditions, thus increasing the Mach number 0.7 performance envelope.

The gains in performance at a Mach number of 0.8 with the addition of plenum suctions capacity is shown in Fig. 18. The shaded area represents the performance envelope with the present PWT-PES capacity. With the addition of a double compressor unit of

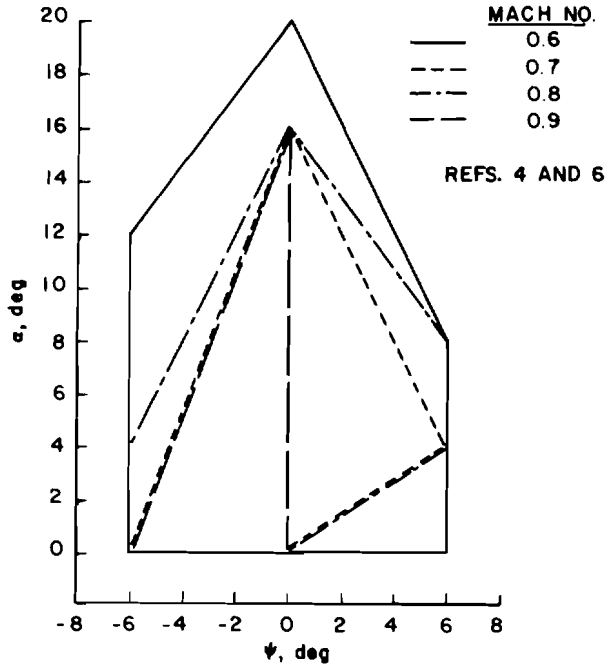

Figure 17. Performance envelope for test inlet/engine with present PWT-16T/PES capability.

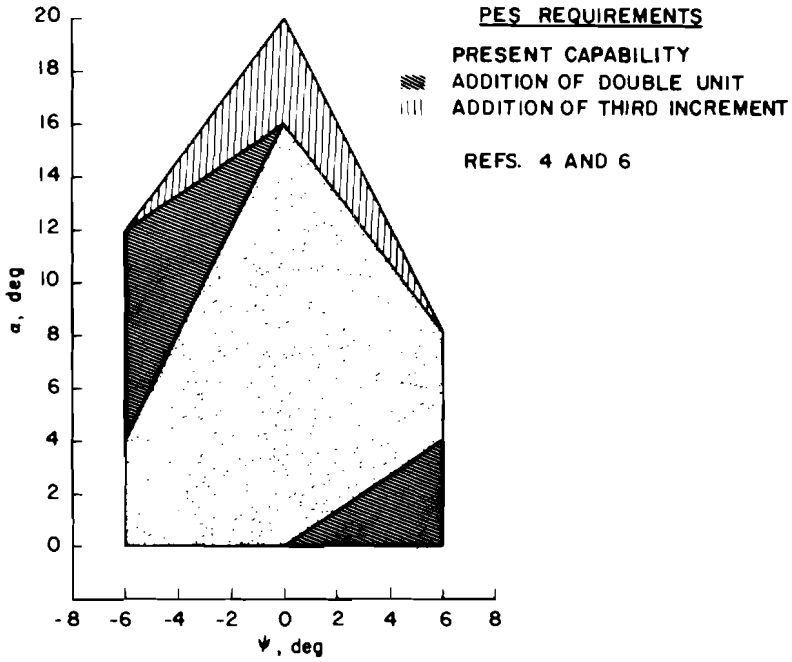

Figure 18. Performance envelope for test inlet/engine in PWT-16T at a Mach number of 0.8.

the type now used, the yaw performance capability can be increased in both the positive and negative direction. With the addition of a third increment (6 units, 3 stages), having the same capacity as one of the present increments, the complete performance envelope can be covered.

The tunnel pressure ratio required to operate with the flow-shaping devices and inlet/engine model installed is shown in Fig. 19. The pressure ratio ranges shown are for the same test conditions that gave the plenum suction requirement range in Fig. 16. The data points, indicated by the circles, that are shown on the figure were taken from recent PWT-16T operation logs and indicate that the wind tunnel can operate at the pressure ratios required. It should be pointed out that at the maximum pressure ratio required at Mach 0.9, the tunnel pressure attainable would represent a pressure altitude of 15,000 ft. At the other three Mach numbers, a tunnel pressure that represents a pressure altitude of sea level is attainable.

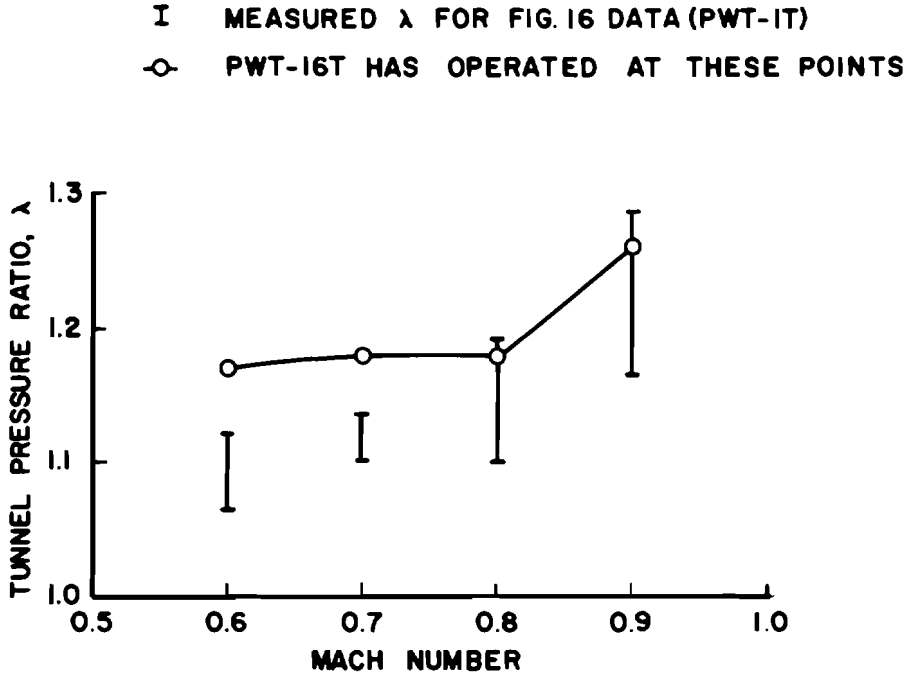

Figure 19. Tunnel pressure ratio requirements with shaping device and inlet/engine installed.

4.0 CONCLUDING REMARKS

Verification of the flow-shaping technique for extending the full-scale inlet/engine testing capability of the AEDC PWT-16T to include simulation of maneuvering conditions has been accomplished (Refs. 4 and 6). The technique has been demonstrated to be feasible

for simulating flight conditions from 0- to 20-deg angle of attack at 0-deg yaw angle, and from 0- to 8-deg angle of attack at ±6-deg yaw angle through a Mach number range from 0.6 to 0.9. Aerodynamic loads on the shaping devices for all simulation conditions have been measured, and the wind tunnel operating characteristics for all simulation conditions have been determined. All data needed to design the necessary support equipment for a workable system are now available. Although a considerable part of the performance envelope is obtainable with the present PWT-PES, to best utilize the technique will require the addition of at least one double unit (same type as now used) to the existing PWT-PES. Finally, the design concept being considered will have transient testing capability over the shaping device rotational range. This could be an aid in tuning the inlet control system if the technique is put into operation.

REFERENCES

1. Palko, R. L. "Full-Scale Inlet/Engine Testing at High Maneuvering Angles at Transonic Velocities." AIAA Paper No. 72-1026. Presented at the AIAA Seventh Aerodynamics Testing Conference, Palo Alto, California, September 13-15, 1972.

2. Palko, R. L. "A Method of Testing Full-Scale Inlet/Engine Systems at High Angles of Attack and Yaw at Transonic Velocities." AIAA Paper No. 72-1097. Presented at the AIAA/SAE 8th Joint Propulsion Specialist Conference, New Orleans, Louisiana, November 29 - December 1, 1972.

3. Palko, R. L. "A Method to Increase the Full-Scale Inlet/Engine System Testing Capability of the AEDC 16-ft Transonic Wind Tunnel." AEDC-TR-73-9 (AD762912), June 1973.

4. Palko, R. L. "Experimental Verification of a Technique for Testing Full-Scale Inlet/Engine Systems at Angles of Attack up to 20 deg at Transonic Speeds." AEDC-TR-73-169 (AD769307), October 1973.

5. Palko, R. L. "Development and Experimental Verification of a Technique to Test Full-Scale Inlet/Engine Systems at Maneuvering Conditions." AIAA Paper No. 74-1199. Presented at the AIAA/SAE 10th Propulsion Conference, San Diego, California, October 21-23, 1974.

6. Palko, R. L. "Experimental Verification of a Transonic Test Technique for Full-Scale Inlet/Engine Systems Simulating Maneuvering Attitudes." AEDC-TR-74-80 (AD787659), October 1974.

APPENDIX A
EFFECT OF MACH NUMBER ON FORCE AND MOMENT COEFFICIENTS

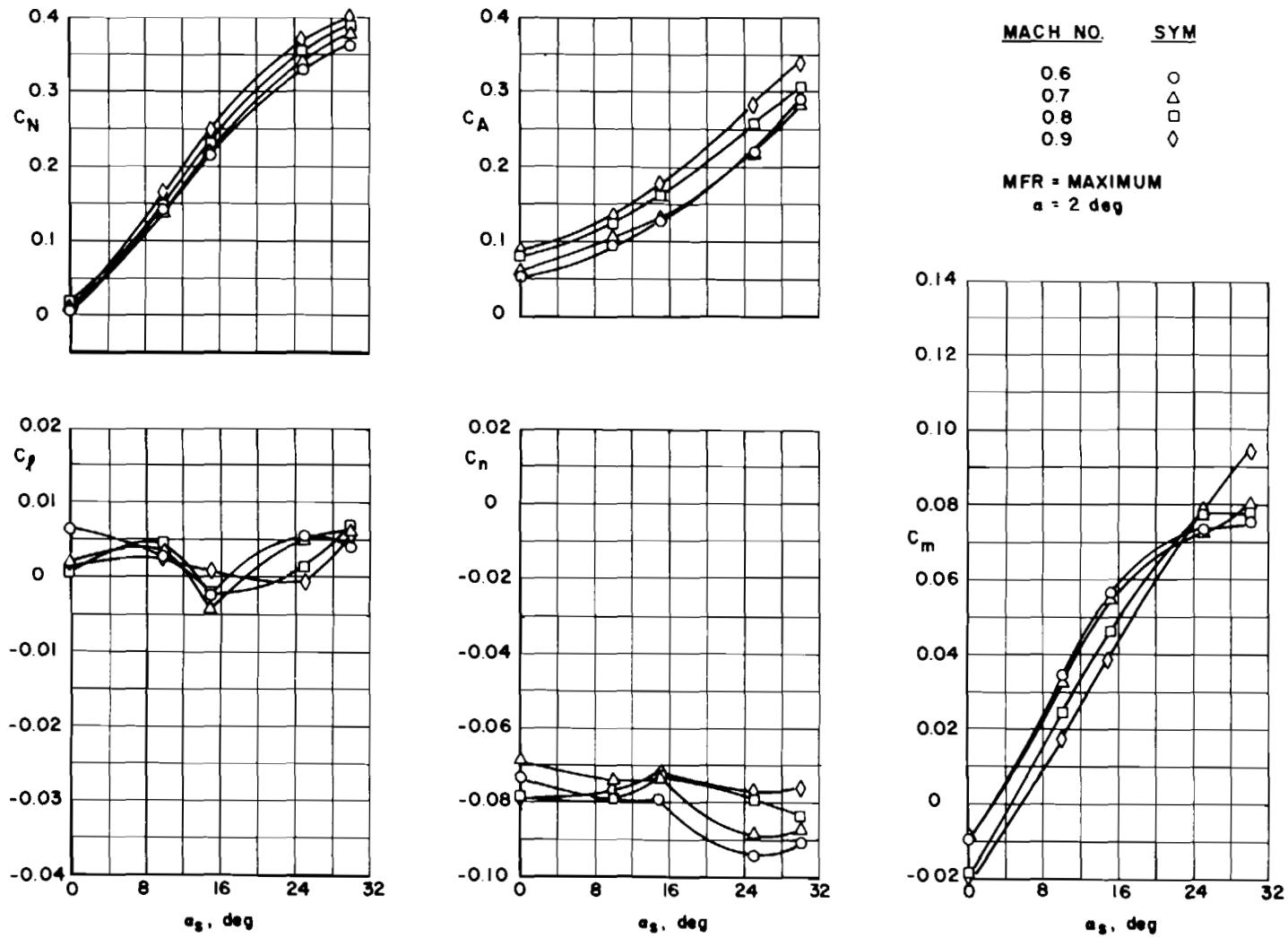

Figure A-1. Effect of Mach number on the force and moment coefficients with the 1MMC2 configuration at β = 10 deg.

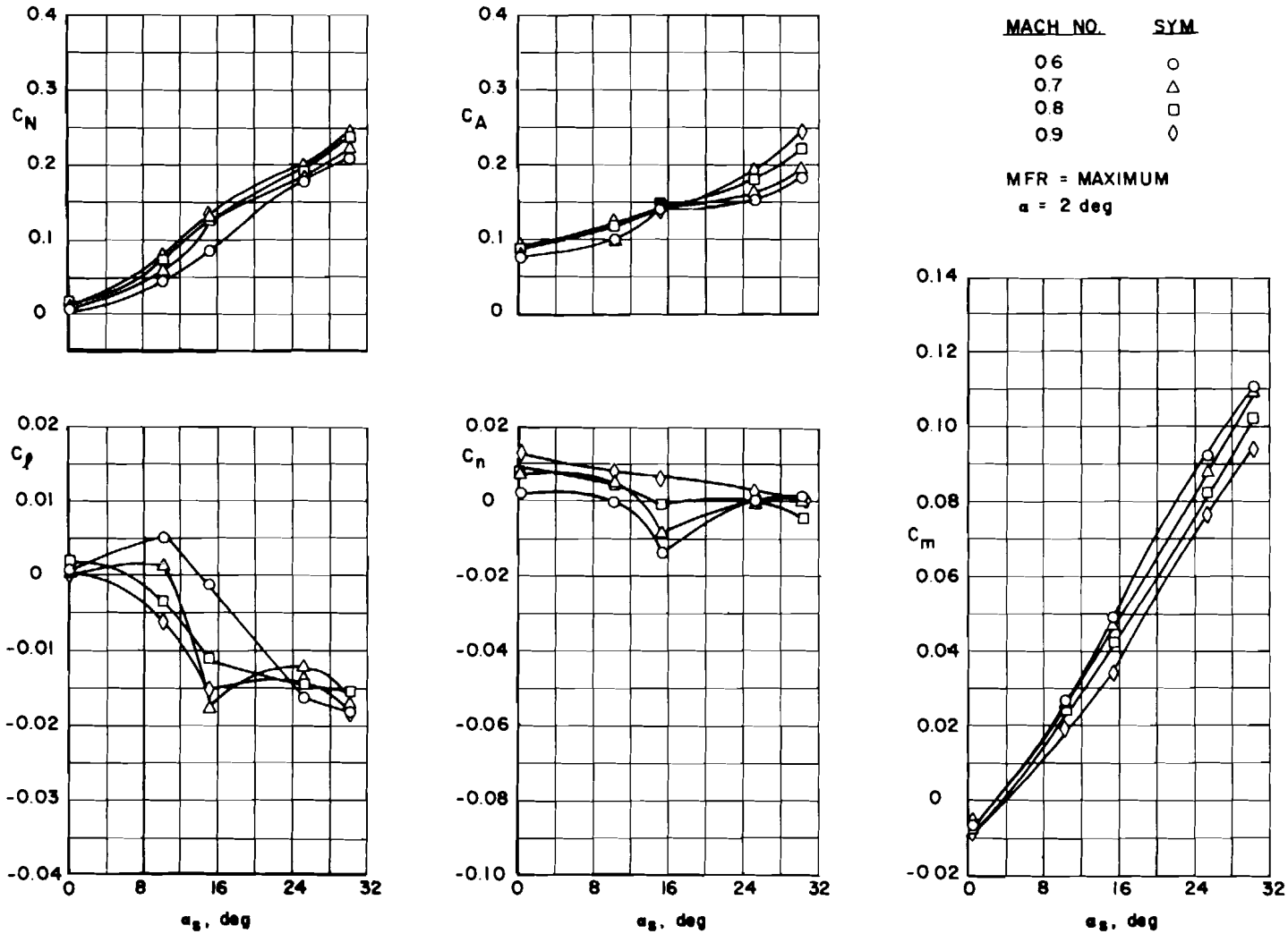

Figure A-2. Effect of Mach number on the force and moment coefficients with the MC configuration at β = 0 deg.

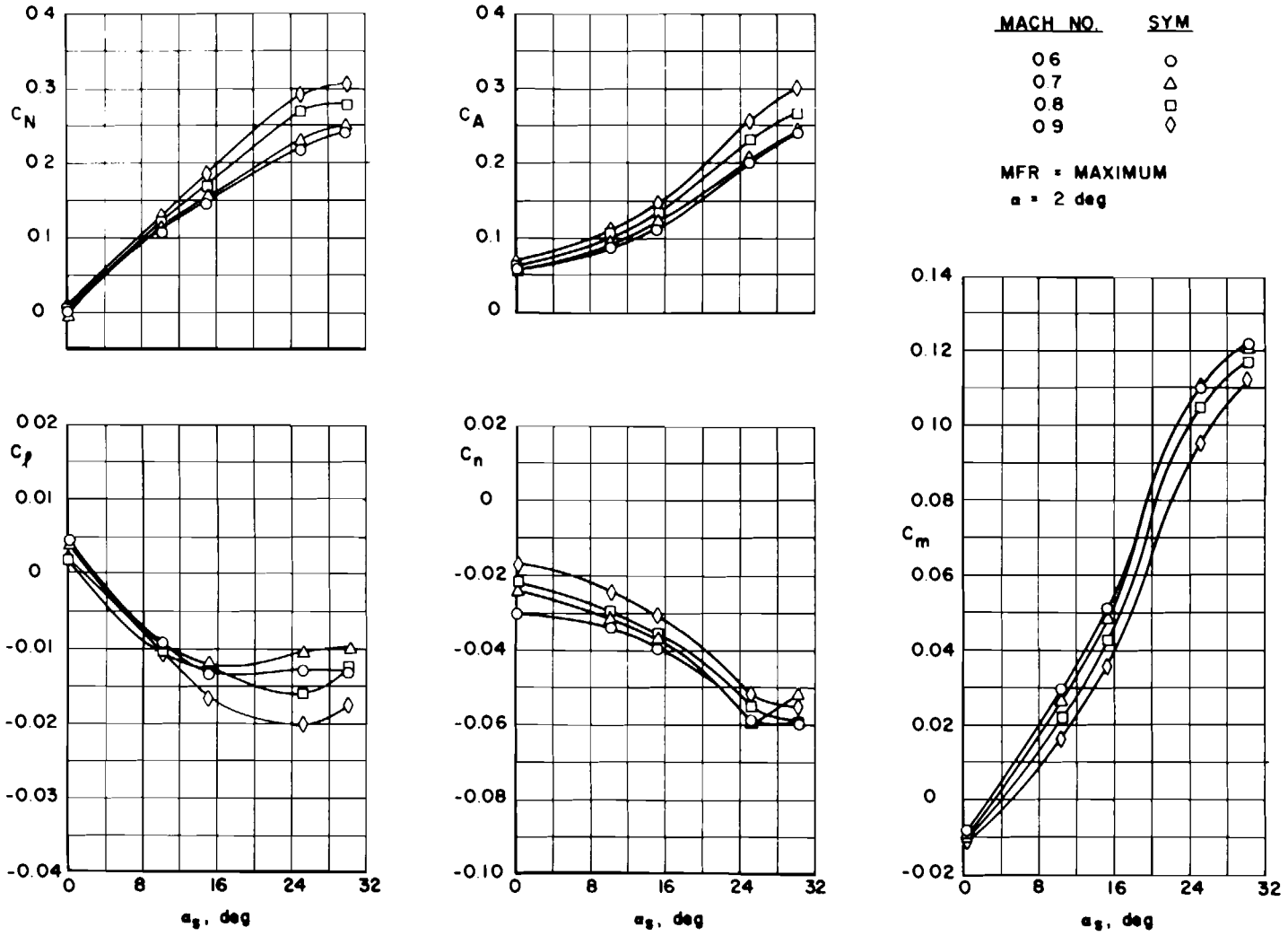

Figure A-3. Effect of Mach number on the force and moment coefficients with the MC configuration at β = 10 deg.

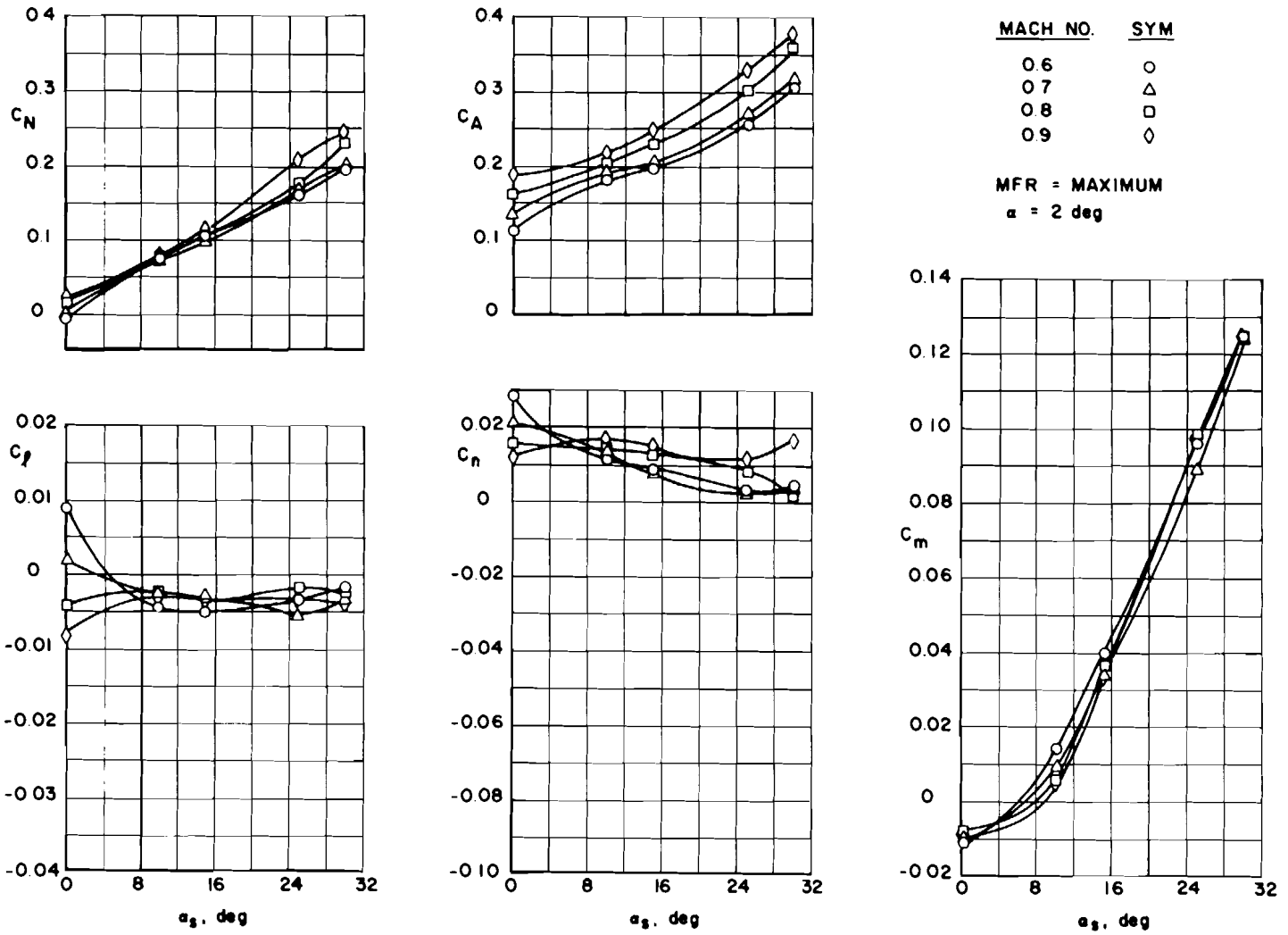

Figure A-4. Effect of Mach number on the force and moment coefficient with the 2MMC configuration at β = 0 deg.

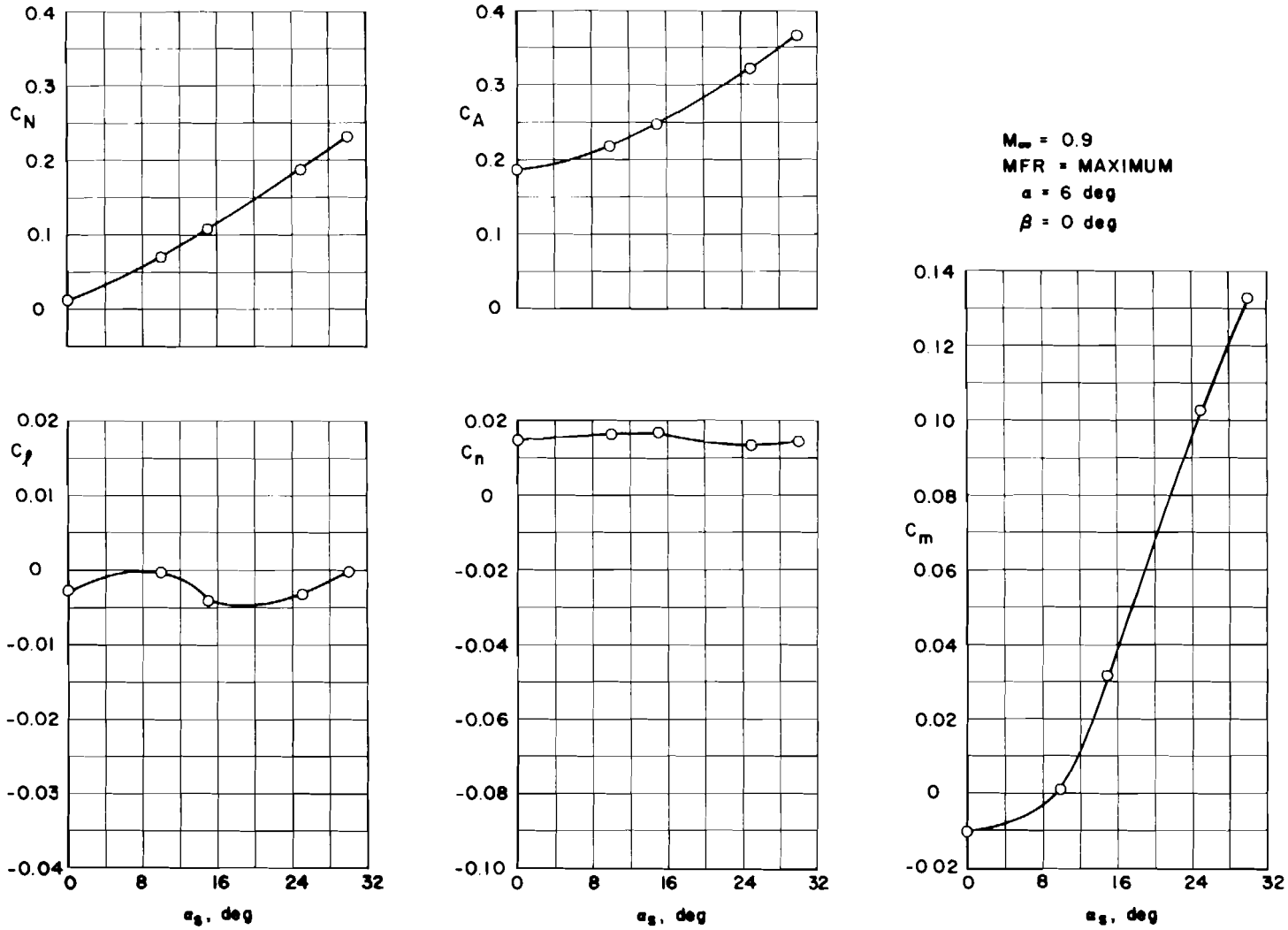

Figure A-5. Force and moment coefficients for test condition that gave maximum pitching moment (2 MMC configuration).

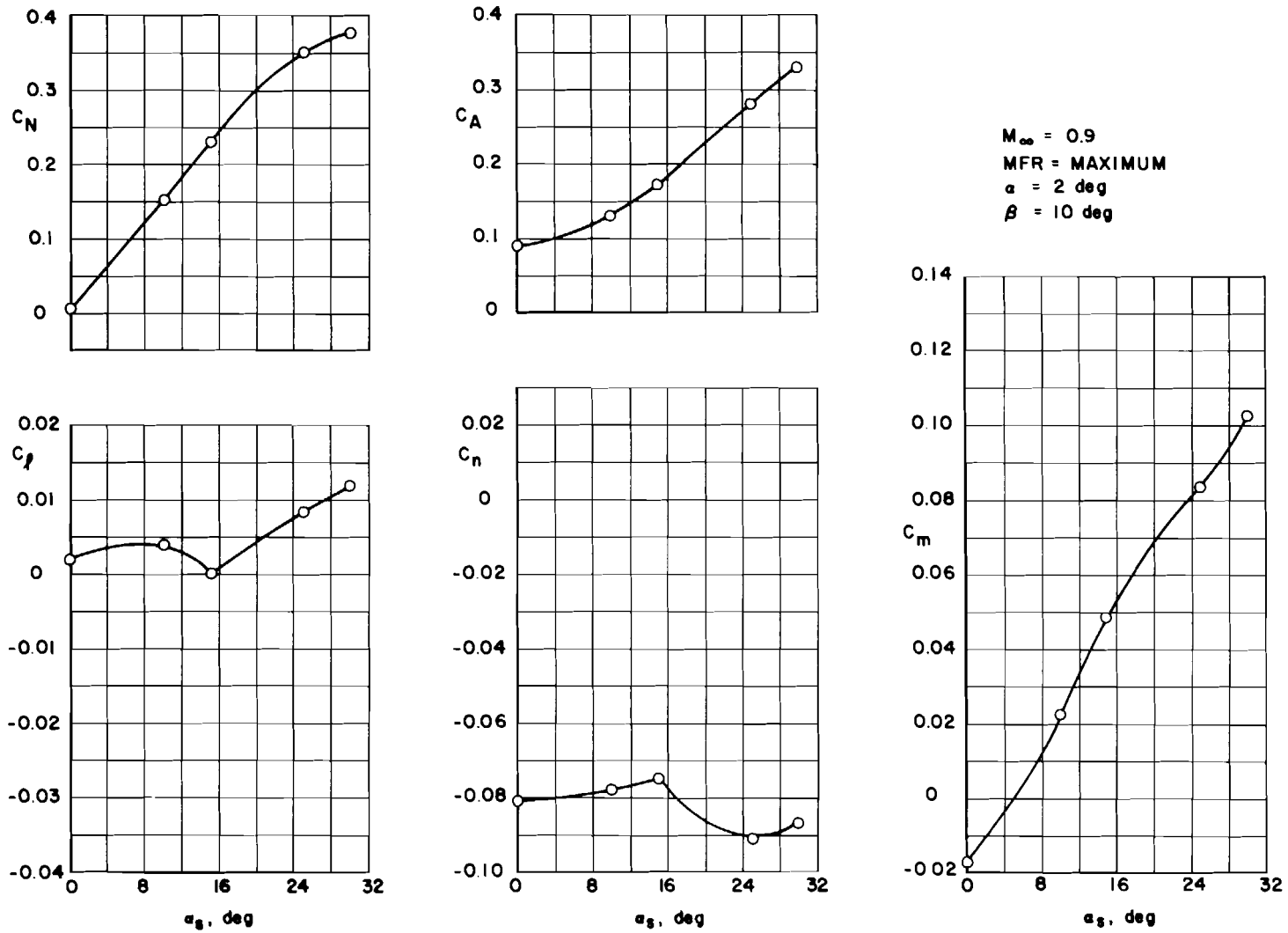

Figure A-6. Force and moment coefficients for test condition that gave maximum yawing moment (1MMC2 configuration).

NOMENCLATURE

b	Reference length, in. (ft), Fig. 3
C_A	Axial-force coefficient, F_A/QS
C_ℓ	Rolling-moment coefficient, M_ℓ/QSb
C_m	Pitching-moment coefficient, $M_m/QS\bar{c}$
C_N	Normal-force coefficient, F_N/QS
C_n	Yawing moment coefficient, M_n/QSb
$\bar{c}$	Reference chord, in. (ft), Fig. 3
F_A	Axial force, lb
F_N	Normal force, lb
MFR	Inlet mass flow ratio, actual mass flow/capture area mass flow
M_ℓ	Rolling moment, in.-lb (ft-lb)
M_m	Pitching moment, in.-lb (ft-lb)
M_n	Yawing moment, in.-lb (ft-lb)
M_∞	Free-stream Mach number
P_t	Free-stream total pressure, psf
Q	Free-stream dynamic pressure, psf
S	Reference area, $in.^2$ (ft^2), Fig. 3
WP/WT	Plenum weight flow/theoretical tunnel weight flow
α	Inlet angle of attack, deg, Fig. 5a
α_s	Shaping device rotation relative to wind tunnel centerline, deg, Fig. 5a
β	Shaping device angle of yaw relative to wind tunnel centerline, deg, Fig. 6
ψ	Inlet angle of yaw, deg